

Size effects of pyroelectric coefficient and dielectric susceptibility in ferroelectric thin films

M.D. Glinchuk and E.A. Eliseev
*Institute for Materials Sciences, NASC of
 Ukraine, Krjijanovskogo 3, 252180, Kiev, Ukraine*

V. A. Stephanovich
*Institute of Mathematics, University of Opole, Oleska 48,
 45-052, Opole, Poland
 (January 8, 2022)*

We calculate the pyrocoefficient, static dielectric susceptibility profiles and its thickness dependence of ferroelectric thin films. Also, the temperature dependences of above quantities have been calculated. For the calculations we use Landau phenomenological theory, leading to Lamé equations. These equations subject to boundary conditions with different extrapolation length on the surfaces have been solved numerically. The divergency of pyroelectric coefficient and static dielectric susceptibility in the vicinity of thickness induced ferroelectric phase transition (i.e. at $l \approx l_c$ or $T \approx T_{cl}$) has been shown to be the most prominent size effect in ferroelectric thin films.

We also calculate the dependence of critical thickness l_c and critical temperature T_{cl} on extrapolation length and film thickness. The latter defines temperature - thickness phase diagram of the film with paraelectric phase at $l \leq l_c$, $T \geq 0$ or $T \geq T_{cl}$ and ferroelectric phase at $l > l_c$ and $T < T_{cl}$. We compare our theory with available experimental data.

I. INTRODUCTION

Ferroelectric thin films attract much attention of the scientists due to important fundamental problems related to size effects resulting in drastic difference between physical properties of the films and of the bulk ferroelectrics (see e.g. [1]). On the other hand in the recent years a lot of efforts have been spared to the application of ferroelectric thin films in pyroelectric and piezoelectric sensors, in some types of random access memory devices, optical memories, microswitches etc. [2,3]. The prospect of these and other applications depends strongly on the solution of fundamental scientific problems of thin films anomalous properties and their dependence on the film thickness. The latter seems to be especially important since the film thickness can be easily adjusted, this adjustment can lead to essential change of the physical properties. In particular, to obtain thin film pyroelectric sensors or capacitors with high performance one has to know the film thickness that gives maximal value of pyrocoefficient or dielectric permittivity respectively. Keeping in mind that recently giant dielectric response (several hundred thousands) was observed in ferroelectric thin film multilayers [4] and its origin was shown to be thickness induced ferroelectric phase transition [5], one can suppose the existence of anomalous dielectric response and other properties peculiarities in the single film with some specially adjusted thickness. The critical thickness corresponding to disappearance of spontaneous polarization (thickness induced ferroelectric phase transition) had been calculated recently in several papers (see e.g. [6,7]) in the framework of phenomenological Landau theory. There are only few

works devoted to dielectric permittivity calculations (see e.g. [8]). To the best of our knowledge there are no calculations of pyroelectric coefficient profile and its thickness dependence in ferroelectric thin films. Besides that, all the calculations were performed in supposition that extrapolation lengths (i.e. boundary conditions) on both film surfaces are the same. This seems to be rough approximation due to different conditions on the film surfaces (e.g. substrate and air). Moreover, the greatest part of calculations of ferroelectric thin films properties were performed numerically mainly for the parameters of BaTiO_3 or PbTiO_3 films (see e.g. [9,10]), which makes it difficult to apply the results for arbitrary ferroelectric film and to extract general features of size effects in the films.

In the present paper we perform the analytical calculations of pyroelectric coefficient and dielectric permittivity in ferroelectric thin film in the framework of the phenomenological theory. The profiles, thickness and temperature dependences of these quantities were obtained by analytical solution of Lamé-type equations with different extrapolation lengths (i.e. different boundary conditions) on the surfaces. The theory predicts the divergency of dielectric permittivity and pyrocoefficient in the film with critical thickness. We compare our theory with available experimental data.

II. THEORY. GENERAL EQUATIONS

In what follows we shall consider a film polarized along z direction normal to the surfaces of the film, i.e. polar-

ization $P \equiv P_z$, $P_x = P_y = 0$. This type of polarization can appear as a result of self-polarization of a film grown under special technological conditions without applica-

tion of an external electric field [11].

In the phenomenological theory $P_z(z) \equiv P$ can be obtained by the minimization of free energy functional

$$F = \int_0^l \left(\frac{\alpha P^2}{2} + \frac{\beta P^4}{4} + \frac{\gamma}{2} \left(\frac{dP}{dz} \right)^2 - PE \right) dz + \frac{\gamma}{2} \left[\frac{P^2}{\delta_1} \Big|_{z=0} + \frac{P^2}{\delta_2} \Big|_{z=l} \right] \quad (1)$$

where $E \equiv E_z$ is an external electric field, l is the film thickness, δ_1 and δ_2 are extrapolation lengths on the film surfaces. The coefficients α , β , γ are those of bulk material renormalized by internal mechanical stresses originated from mismatch of substrate and film lattice constants, expansion coefficients, growth imperfections (see [12,5]) and depolarizing field. Since this renormalization can result into transformation of first order phase transition into that of a second order [12], Eq.(1) can be valid for the materials both with first and second order bulk phase transition.

03/03/01

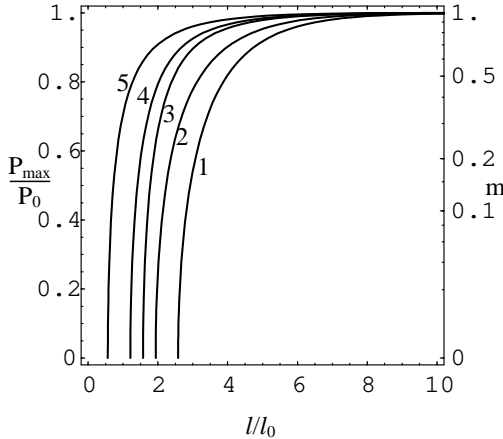


FIG. 1: The thickness dependence of P_{max} and m for several values of extrapolation length. Curves 1, 2, 3, 4 and 5 correspond to extrapolation lengths $(\delta_{01}, \delta_{02}) = (0.1, 0.5)$, $(0.1, 2)$, $(0.1, 10)$, $(0.5, 10)$ and $(2, 10)$ respectively. Arrows correspond to critical thickness.

The minimization of the functional (1) implies following Euler-Lagrange equation

$$\frac{\partial F}{\partial P} - \frac{d}{dz} \frac{dF}{dP'} = 0, P' \equiv \frac{dP}{dz} \quad (2a)$$

and boundary conditions

$$\frac{dP}{dz} \Big|_{z=0} = \frac{P}{\delta_1} \Big|_{z=0}; \quad \frac{dP}{dz} \Big|_{z=l} = - \frac{P}{\delta_2} \Big|_{z=l} \quad (2b)$$

It is seen from Eqs.(2b) that extrapolation lengths determine the crossing points z_1 and z_2 between z axis and tangent lines to $P(z)$ curve at the points $z = 0$ and $z = l$

respectively, i.e. $\delta_1 = -z_1$ and $\delta_2 = z_2 - l$. From this geometric definition of δ_1 and δ_2 one can see that $\delta_1 > 0$, $\delta_2 > 0$ when polarization on the surfaces is smaller than that in the film and both δ_1 and δ_2 are negative in opposite case. Since the conditions on two surfaces can be strongly different (e.g. substrates, electrodes etc.) it may be possible to have different signs of δ_1 and δ_2 , e.g. $\delta_1 > 0$ if $P(z=0) < P(z)$ and $\delta_2 < 0$ if $P(z=l) > P(z)$. In what follows we shall consider the case $\delta_1 > 0$, $\delta_2 > 0$. Eqs. (1) and (2a) lead to the following equation for equilibrium inhomogeneous polarization in the film:

$$\alpha P + \beta P^3 - \gamma \frac{d^2 P}{dz^2} - E = 0 \quad (3)$$

which has to be solved subject to the boundary conditions (2b).

Since $\alpha = \alpha_0(T - T_c)$, where T_c is the temperature of ferroelectric phase transition of the thick film (see e.g. [5]), inhomogeneous polarization of the film $P(z)$ has to depend on T and E . This lead to inhomogeneous pyrocoefficient $\Pi(z) = (dP(z)/dT)_{P=P_s}$ and linear dielectric susceptibility $\chi(z) = (dP(z)/dE)_{P=P_s}$ where P_s is spontaneous polarization defined by Eq.(3) at $E = 0$ and boundary conditions (2b). The differentiation of Eqs. (3) and (2b) gives following differential equations for pyrocoefficient and dielectric susceptibility

$$(\alpha + 3\beta P_s^2)\Pi - \gamma \frac{d^2 \Pi}{dz^2} + \alpha_0 P_s = 0; \quad (4a)$$

$$\frac{d\Pi}{dz} \Big|_{z=0} = \frac{\Pi}{\delta_1} \Big|_{z=0}; \quad \frac{d\Pi}{dz} \Big|_{z=l} = - \frac{\Pi}{\delta_2} \Big|_{z=l} \quad (4b)$$

$$(\alpha + 3\beta P_s^2)\chi - \gamma \frac{d^2 \chi}{dz^2} - 1 = 0; \quad (5a)$$

$$\frac{d\chi}{dz} \Big|_{z=0} = \frac{\chi}{\delta_1} \Big|_{z=0}; \quad \frac{d\chi}{dz} \Big|_{z=l} = - \frac{\chi}{\delta_2} \Big|_{z=l} \quad (5b)$$

The Eqs. (4a) and (5b) define, respectively, pyroelectric coefficient and dielectric susceptibility profiles, i.e. $\Pi(z)$ and $\chi(z)$, as well as their dependences on temperature and thickness of the film. Mean values of pyroelectric coefficient $\bar{\Pi}$ and dielectric susceptibility $\bar{\chi}$ can be calculated as follows

$$\bar{\Pi} = \frac{1}{l} \int_0^l \Pi(z) dz, \quad \bar{\chi} = \frac{1}{l} \int_0^l \chi(z) dz. \quad (6)$$

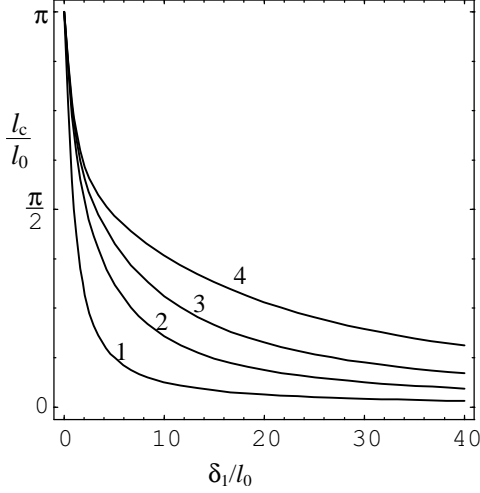


FIG. 2. The dependence of the critical thickness on the extrapolation length. Curves 1, 2, 3 and 4 correspond to $\delta_{02} = \delta_{01}$, $\delta_{02} = 0.2 \delta_{01}$, $\delta_{02} = 0.1 \delta_{01}$ and $\delta_{02} = 0.05 \delta_{01}$ respectively.

III. INHOMOGENEOUS SPONTANEOUS POLARIZATION

Spontaneous polarization can be found by solution of Eq.(3) at $E = 0$ with boundary conditions (2b). In di-

mensionless variables

$$P_1 = \frac{P_z}{P_0}, z_1 = \frac{z}{l_0}, l_1 = \frac{l}{l_0}, \delta_{01,2} = \frac{\delta_{1,2}}{l_0}, \quad (7a)$$

where $l_0 = \sqrt{-\gamma/\alpha}$, $P_0 = \sqrt{-\alpha/\beta}$ ($\alpha = \alpha_0(T - T_c)$, $T \leq T_c$) is the homogeneous polarization of a thick film (where the contribution of gradient can be neglected), the equation for spontaneous polarization of thin film has the form:

$$\frac{d^2 P_1}{dz_1^2} - P_1 - P_1^3 = 0 \quad (7b)$$

The solution of this nonlinear equation subject to above boundary conditions can be written in terms of elliptic sine (sn(...)) (see e.g. [14,15])

$$P_{1z} = \sqrt{\frac{2m}{1+m}} \text{sn} \left(\frac{z_1 + z_0}{\sqrt{1+m}}, m \right) \quad (8)$$

where m and z_0 are the parameters defined by the boundary conditions and film thickness.

In particular, value of z_0 can be obtained from Eqs. (8) and (2b) at $z_1 = 0$. It can be written as

$$z_0 = \sqrt{1+m} F(\arcsin(f_1), m) \quad (9)$$

Values of parameter m can be found from the equation

$$l_1 = 2\sqrt{1+m} (2K(m) - F(\arcsin(f_1), m) - F(\arcsin(f_2), m)) \quad (10)$$

Here

$$f_i \equiv f(m, \delta_{0i}) = \sqrt{\frac{1+m}{2m} \left(1 + \frac{1}{\delta_{0i}^2} - \sqrt{\left(1 + \frac{1}{\delta_{0i}^2} \right)^2 - \frac{4m}{(1+m)^2}} \right)} \quad (11)$$

Note, that to obtain Eq.(10) we used Eqs. (8) and (2b) at $z = l$. In Eqs.(9,10) $K(m)$ and $F(\varphi, m)$ are complete and incomplete elliptic integrals of the first kind respectively [14,15]. The Eqs. (8)-(11) are general formulas for calculation of inhomogeneous polarization of ferroelectric thin films.

It should be noted, that nontrivial solution of equation (3) in the temperature region $T > T_c$ and zero external field $E = 0$ can not satisfy boundary conditions (2a) with positive extrapolation lengths, so only trivial solution $P_s = 0$ is possible in this case.

IV. THICKNESS INDUCED FERROELECTRIC PHASE TRANSITIONS

The analysis of Eq.(10) has shown that values of m lie in the interval $[0, 1]$, $m = 1$ being the value for thick film. We report maximal polarization and m values (respectively on left and right side scales) on Fig.1 as the functions of a film thickness. One can see that at $l/l_0 \approx 8P_m \approx P_0$, i.e. maximal polarization in the film is close to that of a thick film. It follows from Eq.(8), that at $m = 0$ polarization equals zero. This situation appears at some critical thickness l_c , that was found from Eqs. (10), (11) at $m = 0$. For the considered case $\delta_{01} \geq 0$, $\delta_{02} \geq 0$. It can be written in the form

$$l_{1c} = \frac{l_c}{l_0} = \left(\pi - \arcsin \left(\frac{\delta_{01}}{\sqrt{1 + \delta_{01}^2}} \right) - \arcsin \left(\frac{\delta_{02}}{\sqrt{1 + \delta_{02}^2}} \right) \right) \quad (12)$$

Eq.(12) represents the dimensionless critical thickness at which thickness induced ferroelectric phase transition occurs, i.e. ferroelectric phase disappears in the films thinner than critical thickness l_c .

One can see from Eq.(12) that maximal value of l_{1c} ($l_{1c} = \pi$) corresponds to $\delta_{01} = \delta_{02} = 0$, i.e. for $P(z)|_{z=0} = P(z)|_{z=l} = 0$ (see Eq. (2b)). Increase of δ_{01} value leads to decrease l_{1c} so that at $\delta_{01,2} \rightarrow \infty$ $l_{1c} \rightarrow 0$. In the limit $\delta_{01} \rightarrow \infty$, $\delta_{02} \rightarrow 0$ (polarization on one of the surfaces equals zero and acquires some maximal value on the other surface) $l_{1c} \rightarrow \pi/2$ (see Eq.(12)). In Fig.2 the values of l_{1c} for intermediate $\delta_{01} \neq \delta_{02}$ are reported. In particular it follows from this Figure that $\delta_{01} = 40$,

$\delta_{02} = 2$ is far enough from the limit $l_{1c} \rightarrow \pi/2$, which can be achieved at smaller δ_{02} values.

The thickness induced ferroelectric phase transition can occur also in the film with some arbitrary thickness $l \neq l_c$ at critical temperature $T = T_{cl}$. Qualitatively this follows from the fact that m depends both on l and T so that $m = 0$ can be obtained at some special (critical) values of film thickness or temperature. Quantitatively T_{cl} as a function of film thickness and extrapolation length can be obtained from Eq.(12) by substituting $l_0 = \sqrt{\gamma/(\alpha_0 T_c(1 - \tau_{cl}))}$, $\tau_{cl} = T_{cl}/T_c$ and $l_c = l$. This transforms Eq.(12) into that for τ_{cl} , namely

$$\lambda \sqrt{1 - \tau_{cl}} = \pi - \arcsin \frac{d_1 \sqrt{1 - \tau_{cl}}}{\sqrt{1 + d_1^2(1 - \tau_{cl})}} - \arcsin \frac{d_2 \sqrt{1 - \tau_{cl}}}{\sqrt{1 + d_2^2(1 - \tau_{cl})}}, \quad (13a)$$

where

$$\lambda = l \sqrt{\frac{\alpha_0 T_c}{\gamma}} = \frac{l}{l_0(T=0)}, d_{1,2} = \delta_{1,2} \sqrt{\frac{\alpha_0 T_c}{\gamma}} = \frac{\delta_{1,2}}{l_0(T=0)} \quad (13b)$$

are renormalized dimensionless thickness and extrapolation lengths (compare (7a) and (13b)). Expression (13a) determines thickness dependence of dimensionless temperature τ_{cl} of thickness induced ferroelectric phase transition. We show it in Fig.3 for several values of d_1 and d_2 . It is seen that the limit of thick film ($T_{cl} \simeq T_c$) for all the curves corresponds to $l \gtrsim 15l_0(T=0)$. However this limit can be achieved for thinner film ($l \gtrsim 2l_0(T=0)$) in the case of large enough d_1 and d_2 (see curve 1). The large $d_{1,2}$ can be related to large $\delta_{1,2}$ and/or T_c values and/or small γ value (small contribution of polarization gradient), which can be the consequence of strong enough ferroelectric phase transition in a thick film. Note that values of critical thickness shown in Fig.1, 2 are given in the units $l_0 = \sqrt{\gamma/(\alpha_0(T_c - T))}$, while in the Fig.3 they are given in the units $l_0(T=0)$.

Therefore ferroelectric phase transition in a film can be reached by variation of the film thickness at some fixed temperature or by changing the temperature of the film with fixed thickness. As a matter of fact the curves in Fig.3 determine phase boundaries between paraelec-

tric and ferroelectric phases in coordinates temperature - thickness of the film. Namely, at $l \leq l_c$ paraelectric phase (polarization $P = 0$) exists for all temperatures, while at $l > l_c$ it can be both ferroelectric phase ($P \neq 0$) at $T < T_{cl}$ and paraelectric phase at $T \geq T_{cl}$.

V. PYROELECTRIC COEFFICIENT AND DIELECTRIC SUSCEPTIBILITY PROFILES AND THICKNESS DEPENDENCE

A. Pyroelectric coefficient

The solution of Eq. (4a) with the boundary conditions (4b) defines the distribution of pyroelectric coefficient Π and has the following form (see Appendix 1 for details):

$$\Pi(x) = C_1^{py} y_1(x) + C_2^{py} y_2(x) + y_3^{py}(x) \quad (13c)$$

where function $y_i(x)$ have the form:

$$y_1(x) = \text{cn}(x, m) \text{dn}(x, m), \quad (14a)$$

$$y_2(x) = \left(x - \frac{1+m}{1-m} E(am(x), m) \right) \frac{y_1(x)}{1-m} + y_0(x) \frac{1+m^2 - m(1+m) y_0^2(x)}{(1-m)^2}, \quad (14b)$$

$$y_3^{py}(x) = -\Pi_m \left(\left(x - \frac{2 E(am(x), m)}{1-m} \right) y_1(x) + y_0(x) \frac{1+m-2m y_0^2(x)}{1-m} \right) \\ \Pi_m = \Pi_0 \frac{\sqrt{2m(1+m)}}{1-m}, \Pi_0 = \frac{dP_0}{dT} \quad (14c)$$

Here Π_0 is a thick film pyroelectric coefficient and the following notations are introduced:

$$x = \frac{z_1 + z_0}{\sqrt{1+m}}, y_0(x) = \text{sn}(x, m).$$

In Eqs.(14b, 14c) $E(\varphi, m)$ and $\text{am}(x)$ are incomplete elliptic integral of the second kind and elliptic amplitude function respectively [14,15]. We give the explicit expressions for C_1^{py} and C_2^{py} in Appendix 1 due to their cumbersome form. These expressions along with Eqs. (13c-14a) define the profile and temperature dependence of pyroelectric coefficient of a thin film.

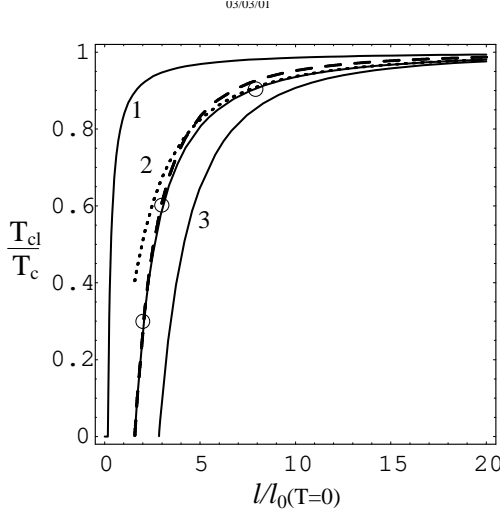


FIG. 3. The thickness dependence of the critical temperature of thickness induced ferroelectric phase transition for different dimensionless extrapolation lengths: $(d_1, d_2) = (10, 15), (2, 0.5), (0.2, 0.1)$ respectively for solid lines 1, 2 and 3. The dashed and dotted lines illustrate the approximate dependencies given by Eqs.(28b) and (28a) respectively with the same parameters as for the curve 2.

This coefficient profiles are reported in Fig.4 for several m values. One can see from Fig.1 that m can be considered as a characteristic of a film thickness: $m \approx 1$ corresponds to the thickest film, while $m \rightarrow 0$ corresponds to the film with critical thickness, i.e. to the thinnest possible film. One can see from Fig.4 that for thick enough films pyroelectric coefficient profile has two maxima in the vicinity of a film surfaces and a flat minimum in the middle part of the film. The value of $\Pi(z)$ in this minimum depends on a film thickness: it is close to pyroelectric coefficient of a thick film for the thickest film (see curves 6 and 7) and it increases with a film thickness decrease (see curve 5) up to complete disappearance of the minimum and its transformation into a flat maximum for some intermediate film thickness (see curves 3, 4). For thinner films pyroelectric coefficient profile has one maximum. Its height and sharpness increases with a film thickness decrease (see curves 1, 2). The strong increase of maximal $\Pi(z)$ value for small m speaks in favour of possible anomaly of pyroelectric coefficient in the film with critical thickness. To check this supposition we performed the calculations of the mean pyroelectric coefficient $\bar{\Pi}$ on the base of Eq.(6). With respect to Eq.(13c) one can write $\bar{\Pi}$ in the following form (see Appendix 2 for details):

$$\bar{\Pi} = C_1^{py} \bar{y}_1 + C_2^{py} \bar{y}_2 + \bar{y}_3^{py} \quad (14d)$$

where mean values of functions $y_i(x)$ have the form:

$$\bar{y}_1 = \frac{f_2 - f_1}{x_2 - x_1}, \quad (15a)$$

$$\bar{y}_2 = \frac{f_2 \left(x_2 - \frac{1+m}{1-m} \left(e_2 - \frac{\sqrt{1+m}}{\delta_{02}} \right) \right) - f_1 \left(x_1 - \frac{1+m}{1-m} \left(e_1 + \frac{\sqrt{1+m}}{\delta_{01}} \right) \right)}{(x_2 - x_1)(1-m)}, \quad (15b)$$

$$\bar{y}_3^{py} = \Pi_m \frac{f_2 \left(2 \left(e_2 - \frac{\sqrt{1+m}}{\delta_{02}} \right) - (1-m)x_2 \right) - f_1 \left(2 \left(e_1 + \frac{\sqrt{1+m}}{\delta_{01}} \right) - (1-m)x_1 \right)}{(x_2 - x_1)(1-m)} \quad (15c)$$

Here the following notations are introduced:

$$x_1 = F(\arcsin(f_1), m), x_2 = 2K(m) - F(\arcsin(f_2), m) \\ e_1 = E(\arcsin(f_1), m), e_2 = 2E(m) - E(\arcsin(f_2), m)$$

and $E(\varphi, m)$ is the complete elliptic integral of the second kind [14,15]. For the sake of illustration we depicted thickness dependence of inverse mean pyrocoefficient $\bar{\Pi}$ in Fig.5 for several δ_{01} , δ_{02} values. One can see that at $l = l_c$ $\Pi_0/\bar{\Pi} \rightarrow 0$, i.e. there is the divergency of pyroelec-

tric coefficient for a film with critical thickness.

Temperature dependence of pyroelectric coefficient in the film with arbitrary thickness can be derived on the base of obtained expressions taking into account that the relation between the film thickness and parameter m (see Eq.(10)) depends on T via parameter $l_0(T) = \sqrt{\gamma/(\alpha_0(T_c - T))} \equiv l_0(\tau = 0)/\sqrt{1 - \tau}$, $\tau = T/T_c$ in variables given by (13b). In these variables Eq.(10) can be rewritten as

$$\lambda\sqrt{1 - \tau} = \sqrt{1 - m} [2K(m) - F(\arcsin(f(m, d_1\sqrt{1 - \tau})), m) - F(\arcsin(f(m, d_2\sqrt{1 - \tau})), m)] \quad (16)$$

This expression defines the temperature dependence of parameter m . This makes possible to calculate the temperature dependence of pyroelectric coefficient on the base of Eq.(14d). The results are reported in Fig.6 by solid lines for several film thickness. The divergency of $\bar{\Pi}(T)$ at $T = T_{cl}$ can be seen, the T_{cl} values for the considered film thickness are marked by open circles in Fig.3.

B. Dielectric susceptibility

Contrary to pyroelectric coefficient that exist only in ferroelectric phase, dielectric response is the property of both ferroelectric and paraelectric phase.

Let us begin with its calculation in ferroelectric phase that exist at $l > l_c$ and $T < T_{cl}$. In such a case it can be calculated similarly to pyroelectric coefficient on the base of Eq.(5a,5b) (see Appendix 1 for details):

$$\chi(x) = C_1^{ch} y_1(x) + C_2^{ch} y_2(x) + y_3^{ch}(x) \quad (17)$$

where

$$y_3^{ch}(x) = -2\chi_0(1 + m) \frac{1 + m - 2m y_0(x)}{(1 - m)^2}, \quad (18)$$

$\chi_0 = -1/2\alpha$ is thick film susceptibility. Coefficients C_1^{ch} and C_2^{ch} differ from C_1^{py} and C_2^{py} in Eq.(13c) because of the difference between $y_3^{py}(x)$ and $y_3^{ch}(x)$ (see Appendix 1). Therefore profiles of dielectric susceptibility can be described by Eq.(17) with respect to Eqs.(14a, 18) and the values of $C_{1,2}^{ch}$ given in Appendix 1.

The dielectric susceptibility profiles calculated on the base of the equation (17) are reported in Fig.7 for several values of parameter m . Comparison of Fig.7 with Fig.4 shows that the profiles of pyrocoefficient and dielectric susceptibility looks qualitatively similar with the same peculiarities of $\chi(z)$ for thicker and thinner films as it was described in previous subsection. However quantitatively the behaviour of $\chi(z)$ for the thinner films differs

from that for $\Pi(z)$: the rate of $\chi(z)$ increase with film thickness decrease is several times larger then the rate of $\Pi(z)$ increase (compare the Figs. 7 and 4). This speaks in favour of statement that dielectric susceptibility is more sensitive to size effects than pyroelectric coefficient. To show that the increase of χ in the thinner film is related to approaching to thickness induced ferroelectric phase transition we performed the calculation of mean dielectric susceptibility $\bar{\chi}$ similarly to $\bar{\Pi}$ calculations (see Eq.(14d))

$$\bar{\chi} = C_1^{ch} \bar{y}_1 + C_2^{ch} \bar{y}_2 + \bar{y}_3^{ch}. \quad (19a)$$

Integration of the third term in Eq.(17) yields following expression (see Appendix 2):

$$\bar{y}_3^{ch} = \frac{\chi_0}{x_2 - x_1} \frac{1 + m}{1 - m} \left(x_2 - x_1 - \frac{2(e_2 - e_1)}{1 - m} \right). \quad (19b)$$

This expression along with Eqs.(15a, 15b) defines the mean value of dielectric susceptibility $\chi(z)$. It is shown on Fig.8 by right branches ($l > l_c$) of solid lines for several values of δ_{01} and δ_{02} . It is seen that at critical thickness marked by arrows $\chi_0/\bar{\chi} = 0$ i.e. $\bar{\chi} \rightarrow \infty$ at $l \rightarrow l_c$ so that we have dielectric susceptibility divergency in the film with critical thickness. Temperature dependence of susceptibility can be calculated with the help of the same formulas (Eq.(16)) keeping in mind that parameter m depends also on temperature. The results of calculations are shown as the left branches ($T < T_{cl}$) of solid lines in Fig.9. The divergency of $\chi(\tau)$ at $\tau = \tau_{cl} = T_{cl}/T_c$ is seen clearly, the values of τ_{cl} in the considered films being marked by open circles in Fig.3. Comparison of pyroelectric coefficient and dielectric susceptibility temperature dependencies (compare Fig.6 and Fig.9) shows that the rate of approaching to infinity as $T \rightarrow T_{cl}$ is smaller for pyroelectric coefficient than for susceptibility and $\chi_0/\bar{\chi}$ is linear function of T/T_c contrary to $\Pi_0/\bar{\Pi}$.

Let us proceed now to calculation of susceptibility in paraelectric phase, i.e. at $l < l_c$ and $T = const$ or $T > T_{cl}$

($T_{cl} \leq T_c$ see Fig.3) and $l = \text{const.}$ In such a case $P_S = 0$ so that Eq.(5a) gives following equation for susceptibility

$$\alpha\chi - \gamma \frac{d^2\chi}{dz^2} = 1, \quad (20)$$

which has to be solved subject to boundary conditions (5b).

The equation (20) is ordinary differential equation of the second order with constant coefficients and its solution can be expressed via trigonometric (when $\gamma/\alpha < 0$) or hyperbolic functions (when $\gamma/\alpha > 0$), while in ferroelectric phase the coefficient of Eq.(5a), including P_S^2 , depends on z and as a result its solution is expressed via elliptic functions rather than simple trigonometric or hyperbolic.

If temperature is less then T_c , the parameter $\alpha =$

$\alpha_0(T - T_c) < 0$ so that $\gamma/\alpha < 0$ and solution of Eq.(20) in dimensionless variables (7a) subject to boundary conditions (5b) has the form

$$\chi(z) = \frac{1}{\alpha} \left\{ 1 + \frac{1}{\Delta_1} [(\cos(l_1) - \delta_{02} \sin(l_1) - 1) \sin(z_1) - (\delta_{02} \cos(l_1) + \sin(l_1) + \delta_{01}) \cos(z_1)] \right\}. \quad (21a)$$

Here

$$\Delta_1 = (\delta_{01} + \delta_{02}) \cos(l_1) + (1 - \delta_{01}\delta_{02}) \sin(l_1) \quad (21b)$$

The expressions (21a, 21b) define the dielectric susceptibility profile in paraelectric phase. Mean value of the susceptibility is found on the base of Eq.(6) and the integration yields:

$$\bar{\chi} = -\frac{1}{\alpha} \left[\frac{2(1 - \cos(l_1)) + (\delta_{01} + \delta_{02}) \sin(l_1)}{l_1((\delta_{01} + \delta_{02}) \cos(l_1) + (1 - \delta_{01}\delta_{02}) \sin(l_1))} - 1 \right]. \quad (22)$$

Thickness dependence described by this expression is reported in Fig.8 by left branches ($l < l_c$) of solid lines for several values of dimensionless extrapolation lengths δ_{01} and δ_{02} . It is seen that $\chi(l \rightarrow l_c) \rightarrow \infty$ while approaching l_c both from paraelectric and ferroelectric phase sides, however the rate of this approaching is different and the value of susceptibility in paraelectric phase is larger than that in ferroelectric phase. Temperature dependence of mean dielectric susceptibility in paraelectric phase can be calculated on the base of Eq.(22) allowing for $l_1 = \lambda\sqrt{1 - \tau}$. The results of calculations are reported in Fig.9 by right branches ($T_c > T > T_{cl}$) of solid lines,

the divergency at $T = T_{cl}$ as well as linear dependence of $\chi_0/\bar{\chi}$ on T/T_c being the characteristic features.

When temperature is larger than T_c (so that $\alpha > 0$, $\gamma/\alpha > 0$), l_0 becomes imaginary so that z_1 and δ_{0i} are also imaginary. In this case the trigonometric functions ($\sin(\dots)$ and $\cos(\dots)$) in the solution (Eq.(21a)) of differential equation (20) convert into hyperbolic functions $i \sinh(\dots)$ and $\cosh(\dots)$. In dimensionless variables (7a) the substitution $-\alpha \rightarrow \alpha$ in Eqs.(21b,22) gives the expressions for distribution of susceptibility χ in paraelectric phase $T > T_c$:

$$\chi(z) = \frac{1}{\alpha} \left(1 + \frac{1}{\Delta_2} \{ [\cosh(l_1) + \delta_{02} \sinh(l_1) - 1] \sinh(z_1) - [\delta_{01} + \delta_{02} \cosh(l_1) + \sinh(l_1)] \cosh(z_1) \} \right), \quad (23)$$

where

$$\Delta_2 = (\delta_{01} + \delta_{02}) \cosh(l_1) + (1 + \delta_{01}\delta_{02}) \sinh(l_1),$$

and mean value of susceptibility $\bar{\chi}$:

$$\bar{\chi} = \frac{1}{\alpha} \left[1 - \frac{2(\cosh(l_1) - 1) + (\delta_{01} + \delta_{02}) \sinh(l_1)}{(\delta_{01} + \delta_{02}) \cosh(l_1) + (1 + \delta_{01}\delta_{02}) \sinh(l_1)} \right], T > T_c. \quad (24)$$

The thickness dependence of mean susceptibility (Eq.(24)) is reported in Fig.10. It is seen from comparison of the Fig.10 and left branches of the solid curves in Fig.8 that $\bar{\chi}$ behaviour in paraelectric phase at $T > T_c$ and at $T_{cl} < T < T_c$ is strongly different: there is neither divergency nor maximum at critical thickness, but

$\bar{\chi}$ increases slowly with thickness increase. As a matter of fact this difference is related to the l_c temperature dependence: $l_c = 0$ at $T > T_c$. It is worth stressing that the considered case $T > T_c$ corresponds to incipient ferroelectric films, which are known to be in paraelectric phase with $T_c = 0$, so that $T_{cl} = 0$ too ($T_{cl} \leq T_c$ by

definition).

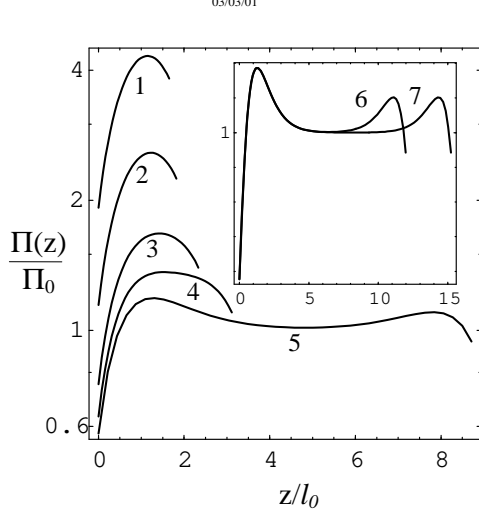


FIG. 4. Pyroelectric coefficient profiles at $\delta_{01} = 0.5$, $\delta_{02} = 2$ for the following m values: 0.04; 0.12; 0.33; 0.57; 0.99; $1 - 10^{-3}$; $1 - 10^{-4}$ respectively for the curves 1; 2; 3; 4; 5; 6; 7.

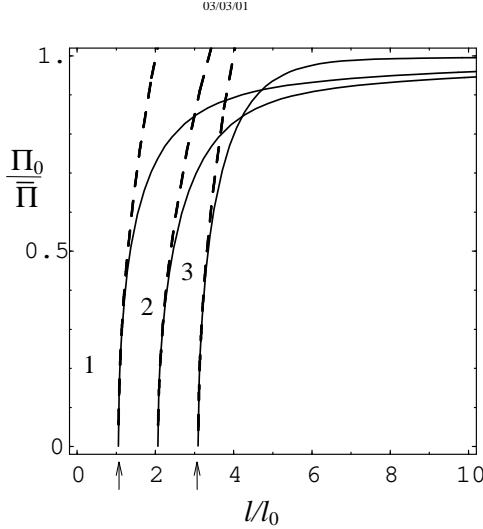


FIG. 5. The thickness dependence of inverse mean pyroelectric coefficient at $T < T_{cl}$ for the following $(\delta_{01}, \delta_{02})$ values: (1.5, 2), (0.6, 0.6) and (0.03, 0.02) for solid curves 1, 2 and 3 respectively. The dashed lines illustrate the description of inverse mean pyroelectric coefficient by the approximate expression (25a) with the same parameters as above. Arrows show the values of critical thickness.

VI. CRITICAL BEHAVIOUR OF PYROELECTRIC COEFFICIENT AND DIELECTRIC SUSCEPTIBILITY

In this section we consider the behaviour of pyroelectric coefficient and dielectric susceptibility in the vicinity of the thickness induced ferroelectric phase transition in a film. This means that we have to calculate the behaviour of these quantities at infinitesimal electric polarization, i.e. parameter $m \rightarrow 0$. On the other hand $m \rightarrow 0$ corre-

sponds to $l \rightarrow l_c$ or $T \rightarrow T_{cl}$.

The calculations can be performed by expansion of expressions (14d) and (19a) for $\bar{\Pi}$ and $\bar{\chi}$ respectively into power series in m up to the first nonvanishing terms. Because of complex form of $\bar{\Pi}(m)$ and $\bar{\chi}(m)$ (see Appendices 1, 2 and expressions (15a, 15b, 15c and 19b)) we put the detailed calculations in Appendix 3. The critical behaviour of dielectric susceptibility while approaching the transition from paraelectric phase is obtained directly from expression (22) that is valid for $T_{cl} \leq T < T_c$. These calculations lead to the following results:

Mean pyroelectric coefficient:

$$\Pi|_{l \rightarrow l_c + 0} = \frac{C_{py}^l}{\sqrt{l_1 - l_{1c}}}, l > l_c, \quad (25a)$$

$$\Pi|_{T \rightarrow T_{cl} - 0} = \frac{C_{py}^T}{\sqrt{\tau_{cl} - \tau}}, T < T_{cl}; \quad (25b)$$

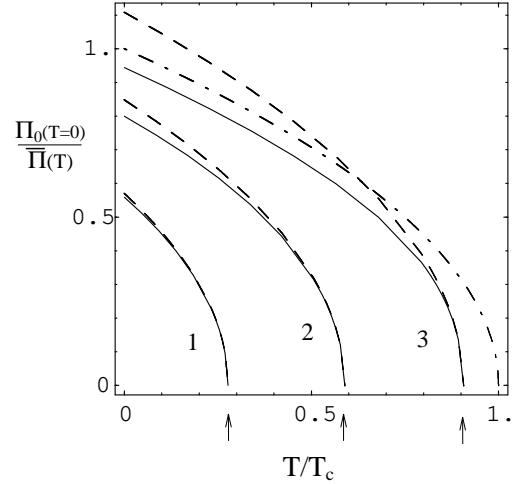


FIG. 6. The temperature dependence of the inverse mean pyroelectric coefficient for the films with following dimensionless thickness $\lambda > \lambda_c$: 2, 3 and 8 (see respectively solid lines 1, 2 and 3) at $d_1 = 0.5$, $d_2 = 2$. The dashed lines illustrate the description of the inverse mean pyroelectric coefficient given by the approximate expression (25b) with the same parameters as above. The dash-dotted line illustrate the dependence of the inverse pyroelectric coefficient of thick film $\Pi_0(T)$. Arrows show the values of critical temperature.

Thickness dependence of mean dielectric susceptibility in paraelectric phase:

$$\bar{\chi}|_{l \rightarrow l_c - 0} = \frac{2C_{ch}^l}{l_{1c} - l_1}, T < T_c, l < l_c, \quad (26a)$$

and in ferroelectric phase:

$$\bar{\chi}|_{l \rightarrow l_c + 0} = \frac{C_{ch}^l}{l_1 - l_{1c}}, T < T_{cl}, l > l_c; \quad (26b)$$

Temperature dependence of mean dielectric susceptibility in ferroelectric phase:

$$\bar{\chi}|_{\tau \rightarrow \tau_{cl}-0} = \frac{C_{ch}^T}{\tau_c - \tau}, l > l_c, T < T_{cl}, \quad (27a)$$

and in paraelectric phase:

$$\bar{\chi}|_{\tau \rightarrow \tau_c+0} = \frac{2C_{ch}^T}{\tau - \tau_c}, l > l_c, T > T_{cl}, \quad (27b)$$

where constants C_{py}^l , C_{py}^T , C_{ch}^l , C_{ch}^T can be found in Appendix 3.

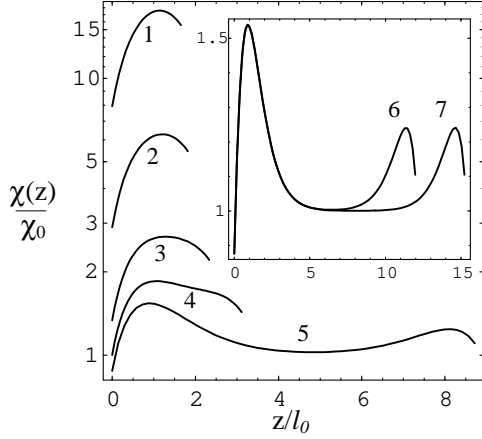


FIG. 7. Dielectric susceptibility profiles in ferroelectric phase for the same parameters as those in Fig.4.

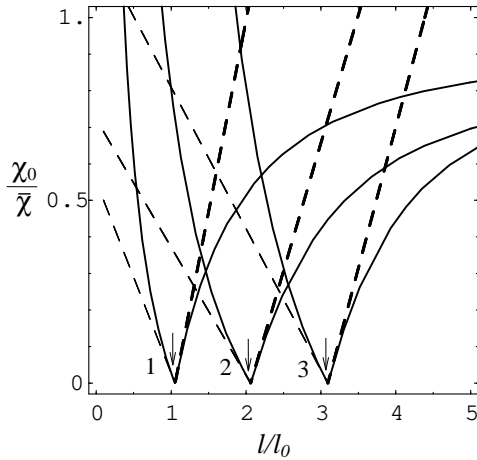


FIG. 8. The thickness dependence of inverse mean dielectric susceptibility at $T < T_c$ for the same parameters as those in Fig.5 (solid lines 1, 2 and 3). The dashed lines illustrate the description of inverse mean dielectric susceptibility given by the approximate expressions (26a,26b). Arrows show the values of critical thickness.

The dependencies given by expressions (25a-27b) are shown by dashed lines in Figs.5, 6, 8 and by crosses in Fig.9. It is seen that for thin enough films the expressions (25b, 27a, 27b) for the temperature critical behaviour, (i.e. in the vicinity of $\tau \approx \tau_{cl}$) describe pretty good the temperature dependence of $\bar{\chi}$ and $\bar{\Pi}$ far enough from these points, while for the thickness critical behaviour

the approximate description (25a, 26a, 26b) is good only in the close vicinity of l_c (see Figs. 5, 8). Note that the lines, corresponding to exact and approximate solutions for curves 1 in Figs. 9 and 6 are almost the same, i.e. approximate formulas perfectly fitted $\bar{\Pi}$ and $\bar{\chi}$ for the most thin films. This is because thickness induced ferroelectric phase transition is typical feature of thin films.

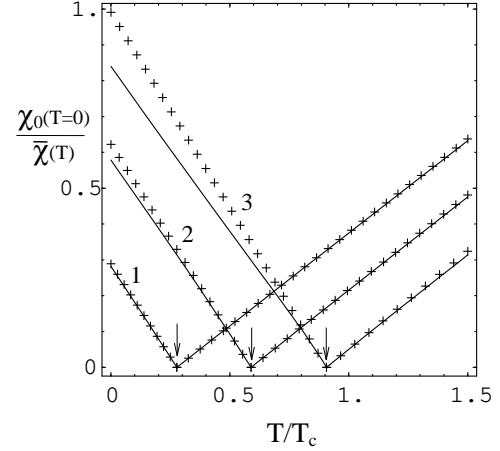


FIG. 9. The temperature dependence of the inverse mean dielectric susceptibility for the films with for the same parameters as those in Fig.6 (solid lines 1, 2 and 3). The crosses illustrate the dependence of inverse mean dielectric susceptibility given by the approximate expressions (29a, b). Arrows show the values of critical temperature.

It is important to emphasize that critical dependence of pyroelectric coefficient (see Eq.(25b)) and dielectric susceptibility (Eq.(27a,27b)) on temperature is similar to that of bulk ferroelectrics.

The critical behaviour of the films with different thickness is related to size effect of transition temperature T_{cl} . This effect is described by expression (13a) and is reported on Fig.3. Formula (13a) can be simplified for thick enough film and for thin films with thickness about critical one, namely

$$\tau_{cl} = 1 - \left(\frac{\pi}{\lambda + d_1 + d_2} \right)^2, \lambda \gg 1 \quad (28a)$$

$$\tau_{cl} = 1 - \left(\frac{\lambda_c + d_1/\sqrt{1+d_1^2} + d_2/\sqrt{1+d_2^2}}{\lambda + d_1/\sqrt{1+d_1^2} + d_2/\sqrt{1+d_2^2}} \right)^2, \quad \lambda - \lambda_c \ll 1 \quad (28b)$$

It is seen from Eqs.(28b) that at $\lambda \rightarrow \infty$, i.e. $l \rightarrow \infty$, $\tau_{cl} \rightarrow 1$, i.e. $T_{cl} \rightarrow T_c$, and at $\lambda \rightarrow \lambda_c$ $\tau_{cl} \rightarrow 0$ in agreement with behaviour shown in Fig.3. It follows also from Fig.3 that thick film limit can be obtained for finite λ values even for small enough $d_{1,2}$ (see curve 3, where $\tau_{cl} \approx 1$ at $\lambda \approx 15$ and $d_1 = 0, 2, d_2 = 0, 1$). To show how the approximate expressions (28b) fit the exact curve (13a) we show them in Fig.3 (for the parameters of curve 2 from that figure) by dotted and dashed lines respectively. One can see the satisfactory agreement between Eqs.(28b) and

the curve 2, the fitting by expression (28b) is better (for all values of λ) than that by Eq.(28a).

VII. DISCUSSION. COMPARISON WITH EXPERIMENT

We performed the analytical calculations of pyroelectric coefficient and dielectric response profiles, their thickness and temperature dependence on the base of solution of differential Lamé equation. The considered boundary conditions include different values of extrapolation lengths on the film boundaries. To our mind this is more adequate for single film (not multilayer structure) than the supposition used in the previous works, where the same extrapolation length (i.e. the same conditions on both boundaries) have been used. In addition, the majority of previous works (see e.g. [8–10]) have been devoted to numerical calculations of the properties of thin films made from BaTiO_3 and PbTiO_3 materials. The analytical expressions for description of size effects of pyroelectric coefficient, dielectric response and polarization in ferroelectric thin films have the advantage of their applicability to any film one can be interested in.

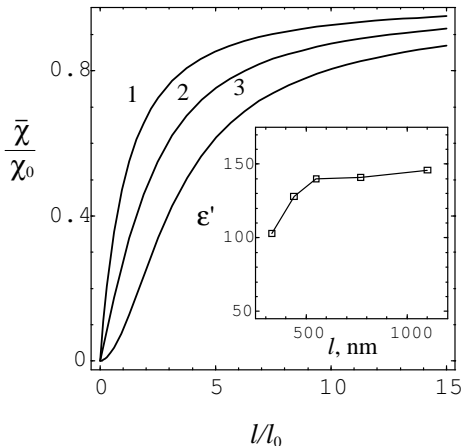


FIG. 10. The calculated thickness dependence of mean dielectric susceptibility at $T > T_c$ for the films with the same parameters as those in Fig.8. The inset shows the observed thickness dependence of real part of permittivity (measured at 100 kHz) of SrTiO_3 film [16].

The theory predicts the divergency of dielectric susceptibility and pyrocoefficient in the vicinity of thickness induced ferroelectric phase transition. Temperature dependence of these quantities can be described by Curie-Weiss law in wide enough temperature range while in thickness domain the same dependencies $\chi \sim 1/|l - l_c|$ and $\Pi \sim 1/\sqrt{l - l_c}$ are valid only in the vicinity of critical thickness l_c . To our mind these simple laws can be in real help for those interested in these properties measurements.

Unfortunately the results of measurements of size effects in ferroelectric thin films are strongly restricted.

This may be related to the difficulties of thin films fabrication (especially with the thickness in the vicinity of l_c that can be several tens nanometers), to the influence of electrodes on the film properties etc. (see e.g. [16]).

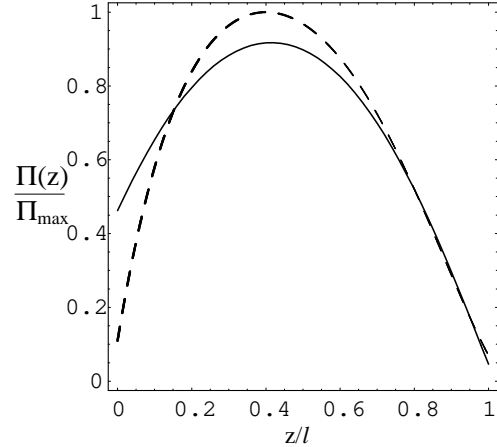


FIG. 11. Pyrocoefficient profile calculated on the base of formulas (13c, 14a) in section 5 at $m = 0.1$; $\delta_{01} = 0.6$, $\delta_{02} = 0.05$ (solid line) and measured in PZT film [18] (dashed line).

To overcome the latter difficulties the application of spectroscopic methods and optical and radiospectroscopy methods in particular seems to be desirable. Special methods are needed also for investigations of the film properties profiles. The most informative is ellipsometry method (see [17] and ref. therein), making possible to measure optic refraction index profile. The calculations of polarization profiles similar to those in Section 3 made it possible to show that measured refraction index profile is related to the film polarization profile [17]. The special laser-intensity-modulation method (LIMM) can be applied to pyrocoefficient profile measurements (see [11,18]). Pyrocurrent coefficient profile extracted in [18] from the pyrocurrent measurement by LIMM in 1 μm thick $\text{PbZr}_{0.75}\text{Ti}_{0.25}\text{O}_3$ film is shown by dashed line in Fig.11. It is seen that it looks really like some of the theoretical curves in Fig.4. Detailed comparison of the theory with experiment is shown in Fig.11 where solid line is theoretical curve with parameters $m = 0.1$, $d_1 = 0.6$, $d_2 = 0.05$. We choose to fit the right "tail" of theoretical curve because of the absence of data related to high frequency measurements so that it can be ambiguities in the experimental points near left "tail" boundaries. However the procedure of pyrocoefficient profile extraction from the measured (in broad frequency range) pyrocurrent implies some numerical methods, the search for the most effective one is still under way (see e.g. [18]). For solution of this problem (that is the essential part of LIMM application to thin films) the calculations of $\Pi(z)$ profile seem to be important. On the other hand, spatial charge is present at the near-electrode layer in real ferroelectric films, that leads to the suppression of the ferroelectric long range order in this region [19]. This phe-

nomenon has not been taken into account in the present work. Therefore both experimental and theoretical approaches need further improvement for the better comparison of the theory with the experiment.

Unfortunately there is no measurements of pyroelectric coefficient thickness dependence. Static dielectric susceptibility thickness dependence measured recently in SrTiO₃ thin films [16]; it is shown on the inset to Fig.10. Since SrTiO₃ is an incipient ferroelectric, i.e. it is in paraelectric phase for all temperatures ($T \geq 0$), $\bar{\chi}$ behaviour is described by Eq. (24) (compare curves in the Fig.10 with those in the inset) pretty good.

The theory prediction about the divergency of pyroelectric coefficient and static dielectric susceptibility in the vicinity of thickness induced ferroelectric phase transition in thin films is waiting for the experimental confirmation.

APPENDIX A:

Let us rewrite the equations (4a) and (5a) for dielectric susceptibility $\chi(x)$ and pyroelectric coefficient $\Pi(x)$ with respect to expression (8) for polarization distribution. Introducing new variable $x = (z_1 + z_0)/\sqrt{1+m}$ and denoting χ and Π as y , one can find following equation for $y(x)$:

$$\frac{d^2 y(x)}{dx^2} + (1+m-6m y_0^2(x)) y(x) = g_y(x), \quad (\text{A1})$$

$$y_0(x) = \text{sn}(x, m)$$

with the boundary conditions

$$\left. \frac{dy(x)}{dx} \right|_{x=x_1} = \frac{\sqrt{1+m}}{\delta_{01}} y(x)|_{x=x_1},$$

$$\left. \frac{dy(x)}{dx} \right|_{x=x_2} = -\frac{\sqrt{1+m}}{\delta_{02}} y(x)|_{x=x_2} \quad (\text{A2})$$

General solution of the equation (A1) (particular case of Lamé equation), is the following [20]:

$$y(x) = C_1 y_1(x) + C_2 y_2(x) + y_3(x) \quad (\text{A3a})$$

$$y_1(x) = \text{cn}(x, m) \text{dn}(x, m) \quad (\text{A3b})$$

$$y_2(x) = y_1(x) \int_0^x \frac{d\tilde{x}}{(y_1(\tilde{x}))^2} \quad (\text{A3c})$$

$$y_3(x) = y_1(x) \int_0^x \int_0^{\tilde{x}} \frac{g_y(\tilde{x}) y_1(\tilde{x})}{(y_1(\tilde{x}))^2} d\tilde{x} d\tilde{x} \quad (\text{A3d})$$

The integral in the expression (A3c) can be easily reduced into a standard form (see [21]), its further substitution to the formula (A3c) gives the explicit form of the second fundamental solution of the equation (A1):

$$y_2(x) = \frac{1}{1-m} \left(\left(x - \frac{1+m}{1-m} E(am(x), m) \right) y_1(x) + \right.$$

$$\left. + y_0(x) \frac{1+m^2-m(1+m)y_0^2(x)}{1-m} \right) \quad (\text{A4})$$

To calculate the integral in the expression (A3d) it is necessary to know the explicit form of the function $g_y(x)$. This function has the form (see Eqs.(4a, 5a)):

$$g_{pi}(x) = -2(1+m)\Pi_0 \sqrt{\frac{2m}{1+m}} y_0(x) \quad (\text{A5a})$$

for the calculation of pyroelectric coefficient $\Pi(x)$ and

$$g_{ch}(x) = -2(1+m)\chi_0 \quad (\text{A5b})$$

for the calculation of dielectric susceptibility $\chi(x)$. After substitution (A5a, A5b) to (A3d) and integration over \tilde{x} and \tilde{x} [21], one can get the following expressions for the inhomogeneous solution of equation (A1):

$$y_3^{py}(x) = -\Pi_m \left(\left(x - \frac{2E(am(x), m)}{1-m} \right) y_1(x) + \right.$$

$$\left. + y_0(x) \frac{1+m-2m y_0^2(x)}{1-m} \right),$$

$$\Pi_m = \Pi_0 \frac{\sqrt{2m(1+m)}}{1-m} \quad (\text{A6a})$$

and

$$y_3^{ch}(x) = -2(1+m)\chi_0 \frac{1+m-2m y_0^2(x)}{(1-m)^2} \quad (\text{A6b})$$

Constants C_1, C_2 are determined from the boundary conditions (A2). Substituting expression (A3a) into (A2), one can obtain the system of linear equations for calculation of C_1 and C_2 . The solution of this system gives following form for constants C_1 and C_2

$$C_1 = \frac{B_1 A_{22} - B_2 A_{21}}{\Delta},$$

$$C_2 = \frac{B_2 A_{11} - B_1 A_{12}}{\Delta},$$

$$\Delta = A_{22} A_{11} - A_{21} A_{12} \quad (\text{A7a})$$

where

$$A_{11} = \frac{\sqrt{1+m}}{\delta_{01}} y_1(x_1) - y_1'(x_1),$$

$$A_{21} = \frac{\sqrt{1+m}}{\delta_{01}} y_2(x_1) - y_2'(x_1),$$

$$A_{12} = \frac{\sqrt{1+m}}{\delta_{01}} y_1(x_2) + y_1'(x_2),$$

$$A_{22} = \frac{\sqrt{1+m}}{\delta_{01}} y_2(x_2) + y_2'(x_2),$$

$$B_1 = y_3'(x_1) - \frac{\sqrt{1+m}}{\delta_{01}} y_3(x_1),$$

$$B_2 = -y_3'(x_2) - \frac{\sqrt{1+m}}{\delta_{01}} y_3(x_2) \quad (\text{A7b})$$

Using the explicit form of solutions $y_1(x)$, $y_2(x)$, $y_3(x)$ (A3b, A4, A6a, A6b), values of x_1 , x_2 and notations for e_1 and e_2

$$\begin{aligned} x_1 &= F(\arcsin(f_1), m), x_2 = 2K(m) - F(\arcsin(f_2), m) \\ e_1 &= E(\arcsin(f_1), m), e_2 = 2E(m) - E(\arcsin(f_2), m) \\ f_i &= \sqrt{\frac{1+m}{2m} \left(1 + \frac{1}{\delta_{0i}^2} - \sqrt{\left(1 + \frac{1}{\delta_{0i}^2} \right)^2 - \frac{4m}{(1+m)^2}} \right)} \end{aligned}$$

it is easy to obtain following expression for A_{ij} and B_i

$$\begin{aligned} A_{11} &= f_1 \left((1+m) \left(1 + \frac{1}{\delta_{01}^2} \right) - 2m f_1^2 \right), \\ A_{12} &= -f_2 \left((1+m) \left(1 + \frac{1}{\delta_{02}^2} \right) - 2m f_2^2 \right), \\ A_{2i} &= \frac{1}{1-m} \left(f_i \frac{\sqrt{1+m}}{\delta_{0i}} \frac{2m + m(1+m)f_i^2}{1-m} + \right. \\ &\quad \left. + A_{1i} \left(x_i - \frac{1+m}{1-m} e_i \right) \right), \end{aligned} \quad (A8)$$

$$\begin{aligned} B_i^{py} &= \Pi_m \left(f_i \frac{\sqrt{1+m}}{\delta_{0i}} \frac{1+m+2m f_i^2}{1-m} + \right. \\ &\quad \left. + A_{1i} \left(x_i - \frac{2e_i}{1-m} \right) \right), \end{aligned} \quad (A9)$$

$$\begin{aligned} B_i^{ch} &= \chi_0 \frac{2(1+m)\sqrt{1+m}}{(1-m)^2 \delta_{0i}} (1+m+2m f_i^2), \\ i &= 1, 2. \end{aligned} \quad (A10)$$

This permits to get final form of coefficients C_1^{py} , C_2^{py} with the help of expressions (A7a, A8, A9) and coefficients C_1^{ch} , C_2^{ch} with the help of expressions (A7a, A8, A10).

APPENDIX B:

Mean pyroelectric coefficient $\bar{\Pi}$ and dielectric susceptibility $\bar{\chi}$ are introduced in the expression (6). After changing of variables in the integrals (6), the mean value of function $g(x)$ can be written as

$$\bar{g} = \frac{1}{x_2 - x_1} \int_{x_1}^{x_2} g(x) dx$$

Using expressions (13c, 17) for $\chi(x)$ and $\Pi(x)$, we can write their mean values as follows

$$\bar{\Pi} = C_1^{py} \bar{y}_1 + C_2^{py} \bar{y}_2 + \bar{y}_3^{py} \quad (B1a)$$

$$\bar{\chi} = C_1^{ch} \bar{y}_1 + C_2^{ch} \bar{y}_2 + \bar{y}_3^{ch} \quad (B1b)$$

To calculate $\bar{\Pi}$ and $\bar{\chi}$ it is necessary to integrate all the solutions of equation (A1) over x . Taking into account

the explicit form (A3b, A4, A6a, A6b) of $y_1(x)$, $y_2(x)$, $y_3(x)$, it is easy to reduce the integrals to the standard form and to find that (see [21])

$$\int y_1(x) dx = y_0(x),$$

$$\begin{aligned} \int y_2(x) dx &= \\ &= \frac{1}{1-m} \left(\left(x - \frac{1+m}{1-m} E(\text{am}(x), m) \right) y_0(x) - \frac{1+m}{1-m} y_1(x) \right), \\ \int y_3^{py}(x) dx &= \\ &= -\Pi_m \left(\left(x - \frac{2E(\text{am}(x), m)}{1-m} \right) y_0(x) - \frac{2y_1(x)}{1-m} \right), \\ \int y_3^{ch}(x) dx &= 2\chi_0 \frac{1+m}{1-m} \left(x - \frac{2E(\text{am}(x), m)}{1-m} \right). \end{aligned}$$

These expressions along with values of x_1 and x_2 permit to get the mean values of $y_1(x)$, $y_2(x)$, $y_3(x)$ in the following form

$$\bar{y}_1 = \frac{f_2 - f_1}{x_2 - x_1}, \quad (B2a)$$

$$\begin{aligned} \bar{y}_2 &= \frac{1}{(x_2 - x_1)(1-m)} \times \\ &\times \left[f_2 \left(x_2 - \frac{1+m}{1-m} \left(e_2 - \frac{\sqrt{1+m}}{\delta_{02}} \right) \right) - \right. \\ &\quad \left. - f_1 x_1 - \frac{1+m}{1-m} \left(e_1 + \frac{\sqrt{1+m}}{\delta_{01}} \right) \right], \end{aligned} \quad (B2b)$$

$$\begin{aligned} \bar{y}_3^{py} &= \frac{\Pi_m}{(x_2 - x_1)(1-m)} \times \\ &\times \left[f_2 \left(2 \left(e_2 - \frac{\sqrt{1+m}}{\delta_{02}} \right) - (1-m)x_2 \right) - \right. \\ &\quad \left. - f_1 \left(2 \left(e_1 + \frac{\sqrt{1+m}}{\delta_{01}} \right) - (1-m)x_1 \right) \right], \end{aligned} \quad (B2c)$$

$$\bar{y}_3^{ch} = \frac{\chi_0}{x_2 - x_1} \frac{1+m}{1-m} \left(x_2 - x_1 - \frac{2(e_2 - e_1)}{1-m} \right). \quad (B2d)$$

1. Ferroelectric phase

For the investigation of behavior of mean pyroelectric coefficient $\bar{\Pi}$ and dielectric susceptibility $\bar{\chi}$ in the vicinity of thickness induced phase transition, we are to expand $\bar{\Pi}(m)$ and $\bar{\chi}(m)$ at $m \rightarrow 0$. Using the series for elliptic integrals [21], one can expand A_{ij} , B_i and \bar{y}_i (see (A8, A9, A10) and (B2a, A3a, B2c, B2d)) to the first nonvanishing terms and obtain following relations

$$\bar{\chi}|_{m \rightarrow 0} = \chi_0 \frac{4 \left(\frac{S_1}{\delta_{01}} + \frac{S_2}{\delta_{02}} \right)^2}{3\Delta_0 l_{1c}} \frac{1}{m} \quad (\text{B3a})$$

$$\begin{aligned} \bar{\Pi}|_{m \rightarrow 0} &= \\ &= \Pi_0 \frac{2\sqrt{2} \left(l_{1c} + \frac{S_1^2}{\delta_{01}} + \frac{S_2^2}{\delta_{02}} \right) \left(\frac{S_1}{\delta_{01}} + \frac{S_2}{\delta_{02}} \right)}{3\Delta_0 l_{1c}} \frac{1}{\sqrt{m}} \end{aligned} \quad (\text{B3b})$$

where

$$S_i = \frac{\delta_{0i}}{\sqrt{1 + \delta_{0i}^2}}, i = 1, 2;$$

$$l_{1c} = \pi - \arcsin(S_1) - \arcsin(S_2)$$

$$\Delta_0 = \left(l_{1c} + \frac{S_1^2}{\delta_{01}} \left(1 + \frac{2}{3} S_1^2 \right) + \frac{S_2^2}{\delta_{02}} \left(1 + \frac{2}{3} S_2^2 \right) \right)$$

The dependence of dimensionless thickness $l_1(m)$ has the form

$$l_1 = \sqrt{1+m} (x_2 - x_1). \quad (\text{B4})$$

The expansion over m gives following relation

$$l_1|_{m \rightarrow 0} = l_{1c} + \frac{3}{4} \Delta_0 m$$

Substitution of this expression into (B3a, B3b) gives the structure of mean pyroelectric coefficient $\bar{\Pi}$ and dielectric susceptibility $\bar{\chi}$ in the vicinity of thickness induced phase transition $l_1 \rightarrow l_{1c} + 0$:

$$\bar{\chi}|_{l_1 \rightarrow l_{1c} + 0} = \frac{C_{ch}^l}{l_1 - l_{1c}}, \quad (\text{B5a})$$

$$C_{ch}^l = \chi_0 \frac{\left(\frac{S_1}{\delta_{01}} + \frac{S_2}{\delta_{02}} \right)^2}{l_{1c}} \quad (\text{B5b})$$

$$\bar{\Pi}|_{l_1 \rightarrow l_{1c} + 0} = \frac{C_{py}^l}{\sqrt{l_1 - l_{1c}}}, \quad (\text{B6a})$$

$$C_{py}^l = \Pi_0 \frac{\sqrt{2} \left(l_{1c} + \frac{S_1^2}{\delta_{01}} + \frac{S_2^2}{\delta_{02}} \right) \left(\frac{S_1}{\delta_{01}} + \frac{S_2}{\delta_{02}} \right)}{\sqrt{3\Delta_0 l_{1c}}} \quad (\text{B6b})$$

The temperature dependence of $\bar{\Pi}$ and $\bar{\chi}$ in the vicinity of the phase transition can also be derived from (B4) and (B3a, B3b) with respect to obvious form of l_1 and δ_{0i} . Introducing new notations

$$\begin{aligned} l_1 &= \lambda \sqrt{1 - \tau}, \lambda = l_1(T = 0), \\ \delta_{0i} &= d_i \sqrt{1 - \tau}, d_i = \delta_{0i}(T = 0), \\ \lambda_c &= l_{1c}(T = 0), \tau = \frac{T}{T_c}, \end{aligned} \quad (\text{B7})$$

and using equation for critical temperature $\tau_{cl} = T_{cl}/T_c$

$$\begin{aligned} \lambda \sqrt{1 - \tau_{cl}} &= \pi - \arcsin \left(\frac{d_1 \sqrt{1 - \tau_{cl}}}{\sqrt{1 + d_1^2 (1 - \tau_{cl})}} \right) - \\ &- \arcsin \left(\frac{d_2 \sqrt{1 - \tau_{cl}}}{\sqrt{1 + d_2^2 (1 - \tau_{cl})}} \right) \end{aligned}$$

we can expand the expression (B4) and get following series up to the first order in m

$$\tau|_{m \rightarrow 0} = \tau_c - \frac{\frac{3}{2} (1 - \tau_{cl}) \Delta_0 (\tau = \tau_{cl})}{\lambda_c \sqrt{1 - \tau_{cl}} + \frac{d_1 \sqrt{1 - \tau_{cl}}}{1 + d_1^2 (1 - \tau_{cl})} + \frac{d_2 \sqrt{1 - \tau_{cl}}}{1 + d_2^2 (1 - \tau_{cl})}} m.$$

Applying this expansion to (B3a, B3b), we can rewrite it as follows

$$\bar{\chi}|_{\tau \rightarrow \tau_{cl} - 0} = \frac{C_{ch}^T}{\tau_{cl} - \tau}, \quad (\text{B8a})$$

$$C_{ch}^T = \frac{2N^2}{\lambda_c \sqrt{1 - \tau_{cl}} D} \chi_0(T = 0), \quad (\text{B8b})$$

$$\bar{\Pi}|_{\tau \rightarrow \tau_{cl} - 0} = \frac{C_{py}^T}{\sqrt{\tau_{cl} - \tau}}, \quad (\text{B9a})$$

$$C_{py}^T = \sqrt{\frac{4D}{3G}} \frac{N}{\lambda_c \sqrt{1 - \tau_{cl}}} \Pi_0(T = 0), \quad (\text{B9b})$$

where

$$N = \frac{1}{\sqrt{1 + d_1^2 (1 - \tau_{cl})}} + \frac{1}{\sqrt{1 + d_2^2 (1 - \tau_{cl})}},$$

$$D = \lambda_c \sqrt{1 - \tau_{cl}} + \frac{d_1 \sqrt{1 - \tau_{cl}}}{1 + d_1^2 (1 - \tau_{cl})} + \frac{d_2 \sqrt{1 - \tau_{cl}}}{1 + d_2^2 (1 - \tau_{cl})},$$

$$G = D + \frac{2}{3} \frac{(d_1 \sqrt{1 - \tau_{cl}})^3}{(1 + d_1^2 (1 - \tau_{cl}))^2} + \frac{2}{3} \frac{(d_2 \sqrt{1 - \tau_{cl}})^3}{(1 + d_2^2 (1 - \tau_{cl}))^2}.$$

2. Paraelectric phase

Mean dielectric susceptibility $\bar{\chi}$ in paraelectric phase (i.e. at temperature above T_c or at $l_1 < l_{1c}$) has the form

$$\bar{\chi} = 2\chi_0 \left(\frac{1}{l_1} \frac{(\delta_{01} + \delta_{02}) \sin(l_1) + 2(1 - \cos(l_1))}{(1 - \delta_{01}\delta_{02}) \sin(l_1) + (\delta_{01} + \delta_{02}) \cos(l_1)} - 1 \right) \quad (\text{B10})$$

Expanding (B10) in terms of $(l_1 - l_{1c})$ one can write the asymptotic form of $\bar{\chi}$ at $l_1 \rightarrow l_{1c}$

$$\bar{\chi}|_{l_1 \rightarrow l_{1c} - 0} = \frac{2C_{ch}^l}{l_{1c} - l_1}, \quad (\text{B11})$$

where C_{ch}^l is given by expression (B5b). Using the temperature dependence (B7) of l_1 and δ_{0i} , it is easy to rewrite (B10) as follows

$$\bar{\chi}|_{\tau \rightarrow \tau_{cl}+0} = \frac{2C_{ch}^T}{\tau - \tau_{cl}}, \quad (\text{B12})$$

where coefficient C_{ch}^T is given by the expression (B8b).

-
- | | |
|--|--|
| <p>[1] D.R.Tilley, Ferroelectric thin films (Gordon and Breach, Amsterdam, 1996)</p> <p>[2] S.L.Swartz, V.E.Wood, Condensed Matter News 1, N5, 4 (1992).</p> <p>[3] H.Tabata, T.Kawai, Appl. Phys. Lett. 70, 321 (1997).</p> <p>[4] Y.Kim, R.A.Gerhardt, A.Erbil, Phys. Rev. B 55, 8766 (1997).</p> <p>[5] M.D.Glinchuk, E.A.Eliseev, V.A.Stephanovich, M.G.Karkut, R.Farhi, cond-mat/0004258.</p> <p>[6] Y.Ishibashi, H.Orihara, D.R.Tilley, J. Phys. Soc. Jap. 67, 3292 (1998).</p> <p>[7] Y.G.Wang, W.L.Zhong, P.L.Zhang, Phys. Rev. B 51, 5311 (1995).</p> <p>[8] B.Qu, W.Zhong, P.Zhang, Phys. Rev. B 52, 765 (1995).</p> | <p>[9] Y.G.Wang, W.L.Zhong, P.L.Zhang, Phys. Rev. B 53, 11439 (1996).</p> <p>[10] C.L.Wang, S.R.P.Smith, L. Phys.: Cond. Matter. 7, 7163 (1995).</p> <p>[11] G.E.Pike, W.L.Warren, D.Dimos, B.A.Tuttle, R.Rames, J.Lee, V.G.Keramidas, J.T.Evans, Appl. Phys. Lett. 66, 484 (1995).</p> <p>[12] N.A.Pertsev, A.G.Zembilgotov, A.K.Tagantsev, Phys. Rev. Lett. 80, 1988 (1998).</p> <p>[13] A.M.Kosevich, A.S.Kovalev, Introduction to nonlinear physical mechanics. (Naukova Dumka, Kiev, 1989).</p> <p>[14] J.Mathews, J.L.Walker, Mathematical Methods of Physics (W. A. Benjamin, N.Y., 1965).</p> <p>[15] M.Abramovitz, A.Stegun, Handbook of Mathematical Functions (National Bureau of standards, 1964).</p> <p>[16] R.Thomas, D.G.Dube, N.N.Kamalasanan, S.Chandra, A.S.Bhala, J. Appl. Phys. 82, 4484 (1997).</p> <p>[17] A.Deineka, M.Glinchuk, L.Jastrabik, G.Suchaneck, G.Gerlach, Phys. Stat. Sol. (a) 175, 443 (1999); M.D.Glinchuk, E.A.Eliseev, A.Deineka, L.Jastrabik, (in press).</p> <p>[18] G.Suchaneck, T.H.Sandner, R.Kohler, G.Gerlach, Integrated Ferroelectrics 27, 127 (1999).</p> <p>[19] A.M.Bratkovsky, A.P.Levanyuk, Phys. Rev. B 61, 15042 (2000).</p> <p>[20] Erdelyi A. et al. Higher Transcendental Functions.-N.Y.: McGraw-Hill Book CO; 1953, V. 3.</p> <p>[21] Gradshteyn I.S. and Ryzhik I.M. Tables of integrals.-Moscow: Fizmatgiz, 1963.</p> |
|--|--|